



AIT Series

Trends in earth observation

Volume 1

Earth observation advancements in a changing world

Edited by Chirici G. and Gianinetto M.

Earth observation advancements in a changing world

Edited by

Gherardo Chirici and Marco Gianinetto

AIT Series: Trends in earth observation



Volume 1 - Published in July 2019
Edited by Gherardo Chirici and Marco Gianinetto
Published on behalf of the Associazione Italiana di Telerilevamento (AIT)
Via Lucca 50
50142 Firenze, Italy

ISSN 2612-7148
ISBN 978-88-944687-1-7
DOI: 10.978.88944687/17

All contributions published in the Volume “Earth observation advancements in a changing world” were subject to blind peer review from independent reviewers.

Publication Ethics and Publication Malpractice Statement
Editors, Reviewers and Authors agreed with Publication Ethics and Publication Malpractice Statement

© 2019 by the authors; licensee Italian Society of Remote Sensing (AIT).
This Volume is an open access volume distributed under the terms and conditions of the Creative Commons Attribution license (<http://creativecommons.org/licenses/by/4.0/>).



Preface

Since 1986 the Italian Remote Sensing Society (Associazione Italiana di Telerilevamento – AIT) aims to disseminate remote sensing culture, disciplines and applications in Italy. Specifically, AIT’s mission is to:

- Create a network of people from Research, Academia and hi-tech Companies interested in analysis, development and application of a wide range of remote sensing methods and techniques;
- Promote and coordinate initiatives to expand the use of remote sensing technologies in Italy and across the European Union;
- Foster the exchange of knowledge and cooperation between its members to “shorten” the chain: research→innovation→new applications/markets→research;
- Support the dissemination of remote sensing methods through the organization of congresses, conferences, working groups, including international thematic courses;
- Represent and take care of scientific and cultural interests in remote sensing for institutions, agencies, companies and similar associations, at national and international level.

Recently, AIT was included in the Italian Copernicus User Forum among the representatives of the IV sector. AIT is also the official Society of the European Journal of Remote Sensing, an open-access scholarly journal published by Taylor & Francis.

Until 1995, AIT was used to organise National Conferences, but in 1997, the Society joined a wider Federal Association (Associazioni Scientifiche per le Informazioni Territoriali e Ambientali - ASITA) related to Cartography, GIS, Topography, Photogrammetry and Remote Sensing, which organises annual national conferences to share and diffuse the Geomatic advancements.

In 2016 AIT decided to bring back its tradition to organize its national conferences with a more distinctive research trait. In addition, always in that year, AIT started to organize its annual International Summer Schools for the exploitation of Copernicus data and programmes.

In this framework, we decided to take the opportunity to create a new book series, officially supported by AIT, entitled *Trends in Earth observation*. These volumes want to present to the readers a snapshot of the state-of-the-art in several different application fields.

I hope that *Trends in Earth observation* can contribute to the scientific progress and the continuous innovation of Earth Observation.

AIT President
Livio Rossi

Contents

Introduction	vii
Remote sensing advancements to support modern agriculture practices	1
1. Using hyperspectral data to differentiate shade coffee varieties with and without rust and other canopy species	2
<i>N. Corona-Romero, J.M. Madrigal Gómez, M. González-Stefanoni</i>	
2. Waiting for “institutional” monitoring services of rice crops by remote sensing: is cadastral parcel the proper reference geometry?	6
<i>G. Corvino, A. Lessio, E. Borgogno Mondino</i>	
3. A plot sampling strategy for estimating the area of olive tree crops and olive tree abundance in a mediterranean environment	11
<i>M. Grotti, N. Puletti, F. Chianucci, W. Mattioli, A. Floris, F. Clementel, C. Torresan, M. Marchi, A. Gentile, M. Pisante, A. Marcelli, P. Corona</i>	
4. Phenology and yield assessment in maize seed crops using sentinel 2 vis’ time series	15
<i>M. Croci, F. Calegari, P. Morandi, S. Amaducci, M. Vincini</i>	
5. Use of Sentinel-2 images for water needs monitoring: application on an industrial tomato crop in central Italy	19
<i>B. Rapi, L. Angeli, P. Battista, M. Chiesi, R. Magno, A. Materassi, M. Pieri, M. Romani, F. Sabatini, F. Maselli</i>	
6. MODIS EVI time series to assess new oil palm plantation dynamics in Borneo	23
<i>S. De Petris, P. Boccardo, E. Borgogno-Mondino</i>	
7. Remote sensing characterization of crop vulnerability to flood	28
<i>T. Pacetti, E. Caporali, M.C. Rulli</i>	
Earth observation for monitoring forest resources and environmental processes	32
8. Tree species classification with Sentinel-2 data in european part of Russia	33
<i>E.A. Kurbanov, O.N. Vorobev, S.A. Menshikov, M.S. Ali</i>	
9. A GIS-based assessment of land cover change in an alpine protected area	37
<i>M. Zurlo, B. Bassano, M. Caccianiga</i>	
10. Presence of European beech in its spanish southernmost limit characterized with Landsat intra-annual time series	41
<i>C. Gómez, P. Alejandro, I. Aulló-Maestro, L. Hernández, R. Sánchez de Dios, H. Sainz-Ollero, J.C. Velázquez, F. Montes</i>	
11. Post-hurricane forest mapping in Bory Tucholskie (northern Poland) using random forest-based up-scaling approach of ALS and photogrammetry- based CHM to KOMPSAT-3 and planetscope imagery	45
<i>P. Wężyk, P. Hawryło, K. Zięba-Kulawik</i>	
12. Forest type classification using morphological operators and Forest PA method	49
<i>M. Ustuner, F. B. Sanli, S. Abdikan</i>	
13. Using Google Earth Engine for the analysis of fog and forest landscape interactions in hyper-arid areas of southern Peru	53
<i>E. Forzini, G. Castelli, F. Salbitano, E. Bresci</i>	
14. Detecting tree hedgerows in agroforestry landscapes	57
<i>F. Chiocchini, M. Ciolfi, M. Sarti, M. Lauteri, M. Cherubini, L. Leonardi, P. Paris</i>	
15. Evaluating accurate poplar stem profiles by TLS	61
<i>N. Puletti, M. Grotti, R. Scotti</i>	
16. Classification of dominant forest tree species by multi-source very high resolution remote sensing data	65
<i>B. Del Perugia, D. Travaglini, A. Barbati, A. Barzagli, F. Giannetti, B. Lasserre, S. Nocentini, G. Santopuoli, G. Chirici</i>	

17. ALS data for detecting habitat trees in a multi-layered mediterranean forest	69
<i>G. Santopuoli, M. Di Febbraro, C. Alvites, M. Balsi, M. Marchetti, B. Lasserre</i>	
18. Creating a map of reforestation on abandoned agricultural lands in Mari El republic using satellite images	73
<i>S. A. Lezhnin, R. L. Muzurova</i>	
19. Monitoring the growth dynamics of water hyacinth (<i>Eichhornia crassipes</i>)	77
<i>J.F. Mas</i>	
20. Long-term comparison of in situ and remotely-sensed leaf area index in temperate and mediterranean broadleaved forests	81
<i>C. Tattoni, F. Chianucci, M. Grotti, R. Zorer, A. Cutini, D. Rocchini</i>	
21. Evaluation of the atmospheric upward thermal emission towards SSS retrieval at L Band	85
<i>A.V. Bosisio, G. Macelloni, M. Brogioni</i>	
22. Use of Sentinel-1 and Sentinel-3 data to initialize a numerical weather model	88
<i>L. Pulvirenti, M. Lagasio, A. Parodi, G. Venuti, E. Realini, N. Pierdicca</i>	

Earth observation for disaster risk and geomorphologic application93

23. Modelling soil erosion in the Alps with dynamic RUSLE-LIKE MODEL and satellite observations	94
<i>M. Aiello, M. Gianinetto, R. Vezzoli, F. Rota Nodari, F. Polinelli, F. Frassy, M.C. Rulli, G. Ravazzani, C. Corbari, A. Soncini, D.D. Chiarelli, C. Passera, D. Bocchiola</i>	
24. Soil degradation mapping using GIS, remote sensing and laboratory analysis in the Oum Er Rbia high basin, middle atlas, Morocco	98
<i>A.El Jazouli, A. Barakat, R. Khellouk, J. Rais</i>	
25. UAV application for monitoring the annual geomorphic evolution of a coastal dune in Punta Marina (Italy)	103
<i>E. Grottoli, P. Ciavola, E. Duo, A. Ninfo</i>	
26. Thermographic characterization of a landfill trough an Unmanned Aerial Vehicle	108
<i>F. Capodici, G. Dardanelli, M. Lo Brutto, A. Maltese</i>	
27. UAV digital photogrammetric analysis for soil erosion evaluation in the Rivo catchment: preliminary results	114
<i>A. Minervino Amodio, P.P.C. Aucelli, G. Di Paola, V. Garfi, M. Marchetti, C.M. Roszkopf, S. Troisi</i>	
28. Exploitation of GNSS for calibrating space-borne SAR for the study of landsubsidence	118
<i>G. Farolfi, M. Del Soldato, S.Bianchini, N. Casagli</i>	
29. Contribution of spatial multi-sensor imagery to the cartography of structural lineaments: case study of the paleozoic massif of Rehamna (moroccan Meseta)	122
<i>I. Serbouti, M. Raji, M. Hakdaoui</i>	

Use of remote sensing for water management and protection126

30. COSMO-SkyMed space data supporting disaster risk reduction	127
<i>F. Lenti, M.L. Battagliere, M. Virelli, A. Coletta</i>	
31. The use of remote sensing for water protection in the karst environment of the tabular middle Atlas/the cause of El Hajeb/Morocco	131
<i>A. Muzirafuti, M. Boualoul, G. Randazzo, S. Lanza, A. Allaoui, H. El Ouardi, H. Habibi, H. Ouhaddach</i>	
32. Analysis of floods, urbanization and morphometry of watersheds in Santo André-Brazil	135
<i>J. Gueiros Fusato, M.C. Valverde</i>	
33. Detection of water bodies using open access satellite data: the case study of Kastoria lake in north-western Greece	139
<i>A. Karagianni</i>	
34. A comparison between UAV and high-resolution multispectral satellite images for bathymetry estimation	143
<i>L. Rossi, I. Mammi, E. Pranzini</i>	
35. Analysis of water bodies under partial cloud conditions using satellite images	147
<i>R. Neware, M. Thakare, U. Shrawankar</i>	
36. Estimating vulnerability of water body using Sentinel-2 images and predictive	

eutrophication models: the study case of Bracciano lake (Italy)	151
<i>C. Giuliani, M. Piccinno, A. Veisz, F. Recanatesi</i>	
Coastal monitoring by remote sensing	156
37. Proneness to future marine inundation of Campania coastal plains (southern Italy) in relation to their subsidence trends assessed by Interferometric SAR techniques	157
<i>G. Di Paola, P.P.C. Aucelli, F. Matano, A. Rizzo</i>	
38. Laser scanner and multibeam integrated survey for the assesment of rocky sea cliff geomorphological hazard	162
<i>S. Guida, N. Corradi, B. Federici, A. Lucarelli, P. Brandolini</i>	
39. Shoreline changes at Sant’Agata river mouth (Reggio Calabria, Italy)	167
<i>G. Barbaro, G. Bombino, V. Fiamma, G. Foti, P. Puntorieri, F. Minniti C. Pezzimenti</i>	
40. Earth observation as an aid to coastal water monitoring: potential application to harmful algal bloom detection	171
<i>C. Lapucci, S. Taddei, B. Doronzo, M. Fattorini, S. Melani, G. Betti, F. Maselli, A. Ortolani, B. Gozzini, C. Brandini</i>	
41. Integrating remote sensing data for the assessments of coastal cliffs hazard: MAREGOT project	176
<i>G. Deiana, M. T. Melis, A. Funedda, S. Da Pelo, M. Meloni, L. Naitza, P. Orrù, R. Salvini, A. Sulis</i>	
42. Coastal monitoring through field and satellite data	181
<i>M.Perna, G. Vitale, C. Brandini, E. Pranzini, B. Gozzini</i>	
Application of remote sensing in urban environments.....	186
43. Remote sensing and urban metrics: an automatic classification of spatial configurations to support urban policies	187
<i>E. Barbierato, I. Bernetti, I. Capecchi, C. Saragosa</i>	
44. Remote sensing of the urban heat island with different spatial and temporal resolutions: analysis by MODIS and LANDSAT imagery	191
<i>S. Bonafoni, C. Keeratikasikorn</i>	
45. Building footprint extraction from VHR satellite imagery using a Deep Learning approach	195
<i>C. Sandu, S. Ghassemi, A. Fiandrotti, F. Giulio Tonolo, P. Boccardo, G. Francini, E. Magli</i>	
46. An integration of VHR OPTICAL and RADAR multiscale images processing data and geographical information system applied to a geo-archeological reconstruction in the Ferrara area	199
<i>L. Damiani, F. Immordino, E. Candigliota</i>	
47. Multitemporal landscape pattern analysis: a quantitative approach to support sustainable land management	203
<i>G. Chirici, P. Rossi, D. Fanfani, D. Poli, M. Rossi, B. Mariolle</i>	

THE USE OF REMOTE SENSING FOR WATER PROTECTION IN THE KARST ENVIRONMENT OF THE TABULAR MIDDLE ATLAS / THE CAUSSE OF EL HAJEB/ MOROCCO

A. Muzirafuti^{1*}, M. Boualoul¹, G. Randazzo², S. Lanza², A. Allaoui¹, H. El Ouardi³, H. Habibi³, H. Ouhaddach³

¹ Team of applied geophysics, Nat Ress. and Heritage, Dept. of Geology, Fac. of Sciences, University of Moualy Ismail, BP. 11201 Zitoune, Meknes, Morocco – (muzansel, abdelhamid.gaig11@gmail.com, boualoul@yahoo.fr)

² Section of Earth Sciences, Dept. of Math and Computer Science, Physical Sciences and Earth Sciences, Univ. of Messina. Via F. Stagno d'Alcontres, 31 98166 - Sant'Agata di Messina, Messina, Italy – (grandazzo, lanzas@unime.it)

³ Team of tec mapping, Dept. of Geology, Fac. of Sciences, University of Moualy Ismail, BP. 11201 Zitoune, Meknes, Morocco - h.elouardi@fsumi.ac.ma, (habibim58, hafida.ouhaddach@gmail.com)

KEY WORDS: Causse of El Hajeb, Water protection, Turbidity, Remote sensing, Karst environment

ABSTRACT:

Deep water bodies constitute the strategic water reserves of Morocco. These natural resources are used in many activities such as irrigation in agriculture, and, more importantly, they are the source of fresh drinking water for the local population. However, these resources are vulnerable to anthropogenic and natural phenomena due to ongoing climate change and the increase in population growth. To contribute to the recent initiative for the protection of the karstic environment of water springs in the Tabular Middle Atlas of El Hajeb, the present research work aims to characterize different karst landforms in Liassic carbonate rocks of the Tabular Middle Atlas in the Causse of El Hajeb, where pollution identified in water samples in this region originates. Satellite imagery (Sentinel-2, Landsat, Terra-ASTER, ASTER-GDEM) and GIS tools were used. Based on surface reflectance of dolomite and limestone, especially in shortwave infrared, we delineated the extent of carbonate rocks and areas with intense human activities. Fractures affecting these Liassic rocks were extracted mechanically and manually after the application of Sobel operator filter in N, S, NE and SW main directions. The results show an improvement and a better understanding of the hydrogeological system of this karst environment, in particular the location of new faults identified in NE-SW and NW-SE fault systems which involve infiltration of surface water and groundwater drainage respectively. The percolation of slightly acidic water through these fractures has gradually created cavities and sinkholes which are believed to be the origin of turbidity observed during the analysis of the water springs.

1. INTRODUCTION

Remote sensing has been used in many environmental studies (Julien, 2018) because of its capacity to provide information rapidly on large and hard-to-reach areas. Recently, many programmes such as ASTER, Landsat and Copernicus Sentinels have provided satellite imagery of both high temporal and spatial resolutions free of charge. These data, combined with ground measurements, can lead to solutions for modern challenges such as climate change, natural hazards and increasing population growth. We used this technology in a region which is both sensitive and vulnerable to these phenomena, the karst environment of the Tabular Middle Atlas (TMA) of Morocco, in order to identify its different surface karst landforms.

The TMA of Morocco contains an important water reservoir, located in Liassic carbonate rocks (dolomite and limestone), used for everyday activities by 4236892 population living in Fez-Meknes region, according to 2014 national census of population in Morocco. Because of its importance and the value it holds in the economy of the region, it has been described as château d'eau (SRAT de la Région Fès Boulemane, 2013). Recent studies conducted in this region (Howell, 2016) show that water quality is deteriorating due to anthropogenic activities and natural processes. The present study proposes the use of earth observation and free available data to map various forms of karst (avens, dolines, poljes...) and fault systems; these are the most fragile hotspots where water from the ground

surface charged with with pollutants can easily infiltrate and reach under groundwater bodies. We intend to answer the question related to the part played by each fault system, in order to find out which one is responsible for the infiltration of surface water and consequently is contributing to the development of sinkholes, shown in figure 3. At the time we want to identify which fault system drains water from the Causse to the basin.

The aim of this study is to enhance the understanding of the hydrogeological system of the TMA by adopting a methodology combining space technology and ground-based field work, in order to identify : (1) the direction of the fault systems involved in water infiltration and in development of different karst landforms, (2) the predominant location of karst landforms responsible for the turbidity and chemicals observed in water springs, and (3) human activities contributing to the degradation of water reservoirs.

2. METHODS AND MATERIALS

2.1 Area of study

The TMA of Morocco is located in the northwest of Morocco, bordered to the north by the Saiss basin, to the southwest by the Hercynian Massif Central and to the west by the pleated Middle Atlas shown in figure 1. It holds an important water reservoir, located in Liassic carbonate rocks (dolomite and limestone). It is characterized by a Mediterranean climate with annual

* Corresponding author

precipitation (rain and snow), varying between 700 mm and 900 mm for the period from 1973 to 2008 at Ifrane. The region is occupied by a large number of water springs, such as Ain Aguemguem, Ain Bittit, Ain Boujaoui, Ain Ribaa, Ain Marrouf, Ain Amjrar, Ain Kadhem, ain Zerouka, and lakes called dayets; these are the easily observable karst landforms created by progressive erosion of limestone by water infiltration along faults.

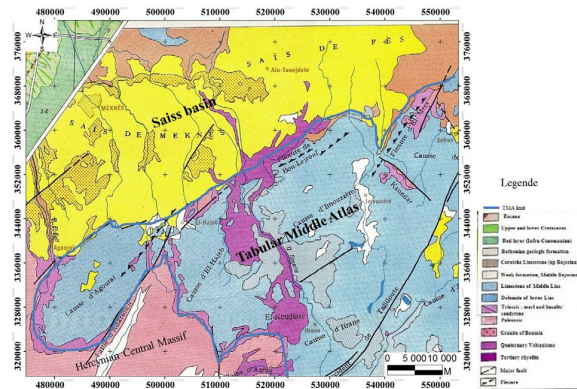


Figure 1: Modified geological stretch map of the TMA

Spectral signatures, shown in figure 2, extracted from Copernicus Sentinel-2 images, show dolomite and limestone with high reflectance in shortwave infrared, vegetation in near infrared and water in blue. Visual interpretation of RGB Sentinel-2 Shortwave Infrared (Band 12,8,4) false color composite image acquired on 10 December 2016 revealed the locations of different geological formations especially carbonate rocks. While principle component analysis was applied to maximize information from a small number of bands (components). In ArcGIS software the high percentage of information observed in response was compared with regional geologic information in order to digitalize linear and curvilinear structures corresponding to lineaments related to both major faults and newly identified fractures. Using Arc Hydro Tool, surface water pathways were extracted on ASTER-DEM; these drainage lines correct precipitations (rain water and snow) from the Causse to the basin and in some cases infiltrate into the ground through fractures.

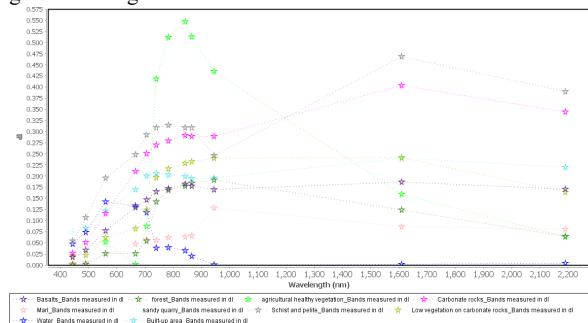


Figure 2 : Spectral signature of land cover objects identified on Sentinel-2 image acquired on 10 December 2016 in TMA

Karst landforms were extracted by subtracting sink-filled and unfilled ASTER-DEM images; we noticed that they are located both on main faults and localized fractures. Agriculture is the most dominant activity in the TMA, mainly in areas occupied by Plio-quaternary geological formations, in some cases in fractured and weathered carbonate rocks.

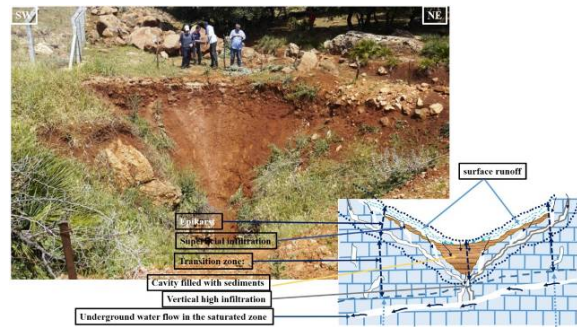


Figure 3: photo of sinkhole taken in the Causse of El Hajeb-Morocco, photograph © 04/05/017.

2.2 Data and software used

In this study we used multi-source satellite images shown in table 1, with Landsat, Terra-ASTER and ASTER-GDEM images downloaded from <https://earthexplorer.usgs.gov> while sentinel-2A images were downloaded from <https://scihub.copernicus.eu>.

Table 1 : Satellite images used

Landsat image				
Acquisition date	Acquisition time	Sensor	Path / Row	
22 May 2016	10 h 57 min 10 sec	L8 (OLI) Level-2	201/37	
Copernicus Sentinel-2A image				
Aquisition date	Acquisition time	Processing level	File Format	
10 December 2016	11h 04min 42sec	Level-1C	JPEG2000, HTML, XML	
Terra-ASTER images				
Aquisition date	Acquisition time	Processing level	Path / Row	
06 August 2000	11h 29min 17sec	Level-1T	201/37	
16 October 2005	11h 07min 47se		201/37	
ASTER-GDEM				
Aquisition date	Entity ID	Spatial Resolution	Map projection	
17 October 2011	ASTERGDEMv2_0N33W006	1 ARC-SECOND	Geographic	

These are free satellite images with high and middle spatial resolution (from 10 to 60 m). Geological maps with a 1:10,000 scale and a 1:50,000 scale, and topographic maps with a 1:50,000 scale were used to calibrate and enhance the classification of satellite images. Free open source software QGIS was used for atmospheric correction, band combination of Landsat 8 and Terra-ASTER while SNAP Desktop was used for atmospheric correction, band combination and image principale component analysis for Sentinel-2A. This Sentinel-2A was further processed and its final results were introduced into ArcGIS 10.3 for layout.

We conducted field work to take structural measurements on basalts and fractured carbonate rocks in order to validate the classification and the location of different karst landforms and fault systems extracted by remote sensing data.

2.3 Data processing and analysis

We adopted a multidisciplinary approach combining multiple sources of data so that we could have sufficient information in our database. We started by geo-referencing topographic and geological maps which gave us a general idea of the area of study. These maps were later compared to satellite images for pixel-based classification.

2.3.1 Satellite imagery pre-processing:

2.3.1.1. Pre-processing and geo-coding:

Our area of study covers a very large surface area which implies utilization of the mosaics of two scenes for Sentinel-2 and one scene for Landsat 8. For Terra-ASTER we used two scenes covering Agourai and El hajeb Causses and Saiss basin. During geo-coding processing the verification of spatial resolution and geometric quality were performed in order to ensure the quality of our database. In the case of geometrical differences between images and maps, control ground points data acquired by Garmin GPS were used to enhance the precision.

2.3.1.2 Pre-processing and geometric adaptation of archive data:

Satellite images, geological and topographic maps were used as reference for calibration and interpretation of archive data such as google images, photographs and open street maps.

2.3.1.3 Pre-processing and atmospheric correction:

Due to the atmospheric conditions and scattered radiance saved by satellite, Dark object subtraction atmospheric correction was performed in QGIS for Landsat 8 OLI and Terra-ASTER images while Sentinel-2 images were atmospherically corrected using Sen2Cor plugin installed in SNAP desktop.

2.3.2. Processing and land cover features extraction:

After the creation of a reliable dataset, optical and RADAR satellite images have been processed in order extract geologic and land cover information.

2.3.2.1. Processing of optical images:

We limited the processing of Landsat 8 OLI and Terra-ASTER images on band combination, shown in table 2, technique for identification of geological formation, Rockwell, 2015, and qualitative landscape interpretation. With spatial resolution of 10 m, 20m and 60 m and spectral resolution of 13 bands, Sentinel-2A images were chosen for geologic and land cover mapping.

Table 2 : RGB band combination used

Satellite	Color affected to the band			RGB image visual interpretation
	Red	Green	Blue	
S-2A	SWIR Band 12	NIR Band 8	Red Band 4	Carbonate rocks appear in pink, Vegetation appears in green, basalts appear in pulpe and water appears in dark blue
L8 (OLI)	SWIR 2 Band 7	NIR Band 5	Red Band 4	Carbonate rocks in appear pink, Vegetation appears in green, basalts appear in dark blue and water appears in blue
Terra-ASTER	VNIR Band 3N	VNIR Band 2	VNI Band 1	Carbonate rocks in appear pink, Vegetation appears in red, basalts appear in dark green and water appears in blue

Object and pixel-based minimum distance supervised classification technique was applied to identify and locate dolomite, limestone, clay and quaternary basalts, agricultural areas, forests, built-up areas, sand quarries, and Paleozoic geological formations with overall accuracy of 96 % and kappa coefficient of 0.86. Normalized difference vegetation index , $NDVI = (\rho_{NIR} - \rho_{RED}) / (\rho_{NIR} + \rho_{RED})$ was computed to provide information on areas occupied by forest, grass, cultivated and uncultivated fields.

In SNAP desktop software, principal component analysis technique, (Loughlin, 1991), was applied on SWIR, NIR and Red bands of Sentinel-2 in order to maximize information in one band. Maximum information was observed in response band resulting from this process. Spatial profile extracted on this response band along the line interpolated on carbonate rocks showed the fluctuation of pixel values with low values on areas of eroded carbonate rocks due to the presence of gradual erosional clays (Terra-rossa) and values were observed on unaltered dolomite. Based on geologic and topographic maps, photointerpretation of changes in these values helped us to identify the continuity of curvilinear or linear structures, such as cracks, faults, fissures and fractures in dolomite and limestone. We also applied direction filter Sobel operator (with 5×5 kernel) on this response band in order to enhance the appearance of curvilinear and linear structures in Nord, South, West, and East directions. Manual digitization and classification of these structures were conducted in ArcGIS to map various fractures of fault systems identified in geological formations.

2.3.2.2. Processing of RADAR (ASTER-GDEM) images:

Advanced Spaceborne thermal Emission and Reflection Radiometer Global Digital Elevation Models (ASTER-GDEM) version 2 with 30 m spatial resolution, acquired on 17 October 2011 was processed in ArcGIS software. We started by extraction elevation information which was later compared to topographic maps to identify depressions, cliffs, valleys, volcanoes, and quarries and slope variation. Like other automatic operators, a photo-interpretation technique was used to identify and locate probable carbonate depressions.

3. RESULTS AND DISCUSSION

Lineaments extracted via satellite images revealed two main fault systems in NW-SE and NS-SW directions shown in table 3. These fractures mainly affect carbonate rocks and play an important role in the hydrogeology system of the region, where they contribute to the infiltration of surface water through the aquifer and also facilitate its movement inside the aquifer.

Table 3 : Direction of main fault systems in TMA

Direction	N-S	E-W	NE-SW	NW-SE
Percentage	20 %	14 %	32 %	27 %

Over one thousand karst landforms, including collapsing and subsidence sinkholes, karst depressions, lakes, pond landscapes, water springs and surface water stream flows, were identified in TMA as shown in figure 4. Their locations on main fault system affecting dolomite and limestone showed that their development is driven by tectonic processes affecting this area.

In order to validate the results obtained from satellite image processing, we conducted field works to take ground-based measurements of fractures and take GPS coordinates of some sinkholes. We took measurements on carbonate rocks and also measurements alongside water springs located in the Tabular Middle Atlas and in its area of contact with the Saiss basin. We found that a large number of sinkholes are located on the NE-

SW fault system, as shown in figure 4, forming a semi-circular axis, while water springs are located on the NW-SE fault system mainly in the area of contact of the TMA and Saiss basin where they are used in irrigation and for drinking water by people living in the Meknes-Fez region. Land cover information obtained from NDVI, shown in table 4, and supervised classification on sentinel-2 shows that in TMA 55 % is occupied by carbonate rocks, 25 % occupied by forest and agricultural areas, while 8 % occupied by basalts and clays.

Table 4 : NDVI and land cover classification

NDVI value	Land cover classification
0.25 <	Carbonate rocks, schists, pelite, basalts and water
0.25 to 0.45	Vegetation spreads on carbonate and schists
0.45 to 0.7	Agriculture vegetation
> 0.7	Dense forest and good healthy vegetation

Agriculture activities conducted on altered and fractured rocks especially basalts and carbonate rocks are believed to be the origin of chemicals products observed in water springs located in the contact of TMA and Saiss basin. In addition the use of fertilizers, pesticides and herbicides for agricultural crops growth modified surface water composition and contribute to dissolution of carbonate rocks.

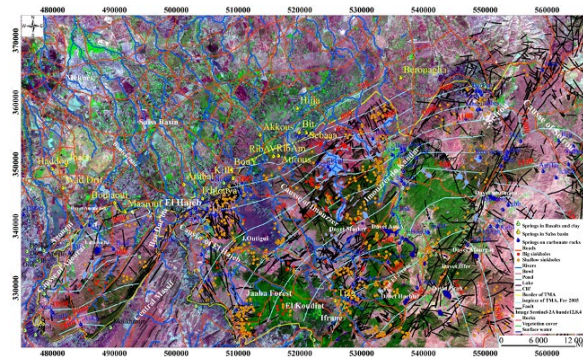


Figure 4: Various karst landforms in Tabular Middle Atlas.

4. CONCLUSION

This study shows the importance of remote sensing and GIS tools. The combination of satellite images and ground-based measurements provides useful information for studies conducted both in large and hard-to-reach areas. We analyzed changes in vegetation using NDVI, changes in surface water, changes in soil minerals and built-up areas using band combinations, and lineament fractures were extracted based on the variation of pixels values on the response of principal component analysis. Karst depressions were extracted manually digitized on ASTER GDEM images.

-Analysis of fractures extracted on satellite images revealed that the NE-SW fault system plays an important role in recharging TMA groundwater aquifers by facilitating the infiltration of surface water from precipitation and melting snow. Many sinkholes and karst depressions are also located along this fault system.

-NDVI and supervised classification results were validated by ground-based measurements taken during our field works and confirmed the location of some collapsing and subsidence sinkholes located near agricultural areas, we also identify geological processes such as dissolution, erosion, and mylonitization affecting fractured carbonate rocks. The

dissolution of dolomite and limestone has created cavities and channels inside these rocks; these channels are the pathway for the movement of groundwater from the TMA to the Saiss basin through NW-SE fault system and can carry with this water erosion products. These products originated either from inside the rocks or from water which has infiltrated from ground surface through sinkholes located on NE-SW faults system.

-The TMA is slightly pleated, creating lowlands and large depressions which people are using for farming activities. The products used to enhance the farming yield, such as fertilizers, pesticides and herbicides, can be mixed with water and change its chemistry, and when they percolate through fissures they have an effect on carbonate rocks because they dissolve them at a fast rate and gradually create underground cavities and sinkholes. In addition, during the period of high precipitation the quantity of water infiltrated becomes high and brings with it more material, leading to the change of water colour mostly observed in water springs. This turbidity affected the health of people using this water.

Human activities are having an impact on the structuration of this karst environment where the quantity of groundwater extracted for irrigation is estimated to be 25 Mm³ per year. On the other hand, ongoing climate change and over-exploitation of water have an impact on aquifer recharge zones by reducing the quantity of precipitation for infiltration and enhancing the evapotranspiration process on the surface, this has contributed to a water loss of 10 Mm³ per year, SRAT de la Région Fès Boulemane, 2013. A protection perimeter around sinkholes identified in agricultural areas is needed in order to reduce human impact on water quality at the same time taking advantage of economic activities conducted in this area.

REFERENCES

- Howell, Brett A., 2016. Spring Responses to Storms and Seasonal Variations in Recharge in the Middle Atlas Region of Morocco. Theses and Dissertations—Earth and Environmental Sciences. P41, http://Uknowledge.uky.edu/ees_etds/41
- Julien Andrieu, 2018. Land cover changes on the West-African coastline from the saloum Delta (Senegal) to Rio Geba (Guinea-Bissau) between 1979 and 2015. European Journal of Remote sensing, 51:1, 314-325
- Loughlin W.P., 1991. Principal component analysis for alteration mapping. Photogrametric Engineering & Remote Sensing, Vol.57, N°9, Sept 1991, pp.1163-1169.
- Rockwell, B.W., Knepper, D.H., Jr., and Hothon, J.D., 2015. Landsat maps (Phase V, deliverable 60), ASTER maps (Phase V, deliverable 62), ASTER_DEM maps (Phase V, deliverable 63), and spectral remote sensing in support of PRISM-II mineral resource assessment project, Islamic republic of Mauritania (Phase V, deliverable 61 and 64).
- Schéma Régional d'Aménagement du Territoire (SRAT) de la Région Fès Boulemane ,2013. Phase 1 : Diagnostic Territorial Stratégique-Etape 1 : Rapports Sectoriels, p29.



This work is licensed under a Creative Commons Attribution-NonCommercial 4.0 International License.